Dear Referee:

Thanks for your careful prompt response on evaluating our manuscript. We appreciate your suggestions and valuable comments, which, we believe, have improved our manuscript. We have carefully considered your comments and revised the manuscript, including the addition of LISA ice speed data for comparison, redrawing Figures 3-7 and the addition of Figure 8, and new context for internal consistency of annual ice velocity data, etc. In the following, we provide point-by-point response to your comments and concerns. For clarity, our responses to the comments are marked in blue.

Sincerely,

Dr. Qiang Shen

Institute of Geodesy & Geophysics, CAS

Wuhan, China

cl980606@whigg.ac.cn

Reply to the Referee #1

Point-by-Point Response

1. Q. …The degree of novelty of this article is low. The same group of authors already published a paper last year using and presenting this velocity data, the validation is not really convincing because they compare to in situ measurements made several decades ago and they totally ignored in their comparison a published Antarctic-wide velocity map derived using the same images (Landsat8).

R. Thank you for your comment. We respectfully disagree on your comment on the low novelty of our manuscript. Our published *Nature Scientific Report Paper* on March 2018 using a previous version of Landsat 8 based Antarctica-wide ice velocity data, which were used to articulate the findings of ice mass loss in Antarctica. In that publication, the details of the prior version of the ice velocity products was concisely described in the supplemental material. Here and in this ESSD manuscript, we describe an updated, validated, and improved version of Antarctica-wide ice velocity data products, including more paired displacement vectors, and improved post-processing method, etc. We believe our manuscript fits ESSD journal's scientific criteria to provide a new, comprehensive data product to the glaciological community for anticipated additional scientific studies.

On the validation of our data product, I am afraid we have made exhaustive studies. In Antarctica, verification of satellite-derived measurements is a challenging task because of its remoteness and extremely cold climate. It is extremely difficult to collect field data synchronously in Antarctica. In the manuscript, we collected nearly all field data for the validation, which is obviously better than those of the previously published papers. Although these in-situ data were measured decadal years ago, they are reasonable for the validation purpose since the ice velocity is relatively stable, especially for the interior of the ice sheet. In addition, for this time we compare our ice velocity results with the LISA750 data according to the Reviewer's advice, the details can be found in main text and following the responses.

2. Q. General comments

1/ The same authors already published a paper using these data in Scientific Reports (https://www.nature.com/articles/s41598-018-22765-0) so the degree of novelty is, at best, incremental. I have much more expectation for an ESSD data in term of originality. More worrysome is the fact that some sections of the submitted manuscript are "copy and paste" from the supplementary text from this earlier publication. I suggest that the editor asks the EGU Copernicus office to produce, if possible, a similarity index between the present article and the supplement of that published study to back up and quantify my comment. The fact that the authors did not cite their earlier work (was it deliberate?) also raises an ethical problem.

R. As stated in response 1, the work is motivated by the purpose of providing a new high-quality data to reuse for glaciological community which is very relevant to the topic of the ESSD journal. The similarity report had been completed before the stage of the open discussion, which our previous paper has been included . We respectfully disagree with the Reviewer that our paper lacks novelty. We undertook an improved post-processing method based on more paired displacement vectors, in the generation of the new and improved Antarctica-wide ice velocity data product. In addition, we had cited our earlier work in dataset repository (htttps://doi.pangaea.de/10.1594/PANGAEA.895738). The earlier work was not cited in main text because we were preparing these two manuscripts at the same time and the earlier work focused on the scientific findings in Antarctic ice sheet. Thanks for your suggestions, we now have cited our earlier work in the abstract and introduction and results sections of the main text. The details can be found in revised manuscript.

3.Q. 2/I find it problematic to have a dataset provided in the format of a commercial software (ENVI). Not the SPIRIT of ESSD I feel. Geotiff raster file should be prefered as they can be read by mean different software open source and commercial.

R. Thank for your comments. In fact, the datasets are provided in the binary format including a header file, which can be opened not just by the commercial software. Anyway, we have updated the datasets in Geotiff format for users to easily read or open the data files.

4. Q. 3/Error assessment. Authors start with a formal error description identifying all sources of errors and then change strategy and just assess the error as the spread in their different velocity fields. But all their velocity fields have priorly been adjusted to the same reference, the slow moving ice in the INSAR velocity mosaic from Mouginot/Rignot, so the spread is, by construction, reduced. If the INSAR mosaic is wrong in these slow moving areas (it includes some artefacts), then all L8 velocity fields will also be wrong. The spread between them will remain small but it does not mean they are accurate.

R. Precise assessment of ice velocity datasets is crucial. However, it is challenging task in Antarctica because its remoteness and harsh climate and environment. The gridded error map of ice velocity is based on a given precision of image coregistration as did in the same manner by Mouginot (2017) /Rignot (2011) and Gardner (2018) For accuracy assessment, we also compared our results with the released ice velocity datasets derived from satellite images and field surveying data. However, there are different time epochs, precise assessment is still difficult. We first investigated the consistence between our results and InSAR, and LISA ice velocity data is now also used for the similar work. The eight profiles of ice velocity datasets show very good consistence (see Figure 3). Second, we investigated our performance of our results by comparing to field surveying measurements. Although these measurements were collected several decades ago, such comparisons are still thought to be reasonable since the ice velocity is slow and stable especially for the interior of the ice sheet, which has been supported by the final comparison results (Figures 5 and 6).

For absolute calibration of ice velocity. Here, we first used the rock data as reference sources, however, it is still difficult to find enough rock places in the interior of ice sheet, therefore, we also used existing SAR ice velocity as a reference to define stable areas (ice velocity <10m/yr) in same manner with LISA data (Gardner et al, 2018). We think that the threshold is relatively rigorous. We assumed that the displacement gradient is stable due to stable image geometry, so only the mean of differences between our ice velocity and InSAR ice velocity is applied for mosaic product. The processing for LISA is similar with our method, but they used the threshold <10m/yr and 10-25m/yr respectively to estimate the offsets caused by geolocation error. Although the processing will lead to that our results and InSAR data will have same performance in slow flowing regions, but our results have also been compared to in-situ measurements and they agree well, which indicate the reliability of our results.

5. 4/ Velocity maps based on Landsat 8 imagery have also been published by another group of authors (Gardner et al., TC, 2018) and a thorough comparison to their results is mandatory. https://www.the-cryosphere.net/12/521/2018/

R. Thank you for your suggestion. Here, our results are also compared to LISA data (lisa750_2013182_2017120_0000_0400_v01) at nearly the same time epochs. The comparison results can be found in revised Figures 3- 6. The detailed analysis can be found in the text of revised manuscript.

Specific comments

6. Q Title : "present day" is too general, Provide dates Time stamp.

R. Thank you for your advice, we have changed the title to 'High-resolution ice velocity data of the Antarctic ice sheet from Landsat 8

7. Q: Problematic to average over 3 summers. Is not it possible to have 3 maps (one per summer) instead (or as an additional product). Would be more useful to user even if they are not complete.

R. Thank you for your advice, we now also provide the two velocity data for individual summer seasons (2014,2015), and they can be available later because it is necessary to submit application of large data files to dataset repository.

8. Q: Robust internal and external validation is too vague

R: As stated in responses 4 to general comments, precise assessment of ice velocity datasets is crucial. However, it is challenging task in Antarctica because its remoteness and harsh climate and environment. The gridded error map of ice velocity is based on a given precision of image coregistration in the same manner with Mouginot/Rignot's and Gardner's ice velocity data. External validation is made by using satellite-derived gridded ice velocity datasets and in-situ measurements, but artifacts is still existing because lack of synchronous in-situ measurement. Here, we deleted the word 'robust'.

9. Q: Be more specific L25 "ice glacier" is not an appropriate terminology

R: it has been changed. Thanks

10. Q: Many spaces missing before the references in the text L41. The 1986 reference is outdated and probably not the best on the topic.

R: Thank you for your comment. They have been changed, and new references have been replaced by AR5 chapter 4 and Ian Joughin et al., 2011.

11. Q L54. It is not "difficult". It is simply impossible..

R: Changed according to your advice, thanks.

12. Q: L56. Missing references about velocity mapping in Antarctica : Bindschadler & Scambos, Science, 1991 ; Scambos et al. RSE 1992 [I see one of them is cited later]

R: The missing references have been now included, they are Bindschadler & Scambos, Science, 1991; Scambos et al. RSE 1992, Scheuchl 2012. Thanks.

13. Q: L61-67. The flow of the introduction is not OK. At these lines authors come back to the reasons why the velocity data are needed. Improve the structure/logics.

R: Sorry for misleading. Thank you for your advice. we edit the part and move it into the back of the first paragraph in introduction . See L47-50 in revised manuscript.

14. Q： L70-71. Cite only reference in Antarctica here.
R: Ok, it has been changed, the References, Joughin et al. 2002, Scambos et al., 1992, Scheuchl et al.,2012 have been added.

15. Q: L76. "most recent" not that "new" now..

R: Thanks, it has been changed.

16. Q:L80. Heid and Kaab did not really work on Antarctica. Cite rather Gardner et al. TC 2018 here

R: Thanks, it has been changed.

17. Q: L109-111. Already stated. Avoid such repetition and go to the point.

R: Thanks. 'using the optical offset method, which will be summarized in Section 2.3' is deleted.

18. Q: L120. "Electronic distance" is a strange method for velocity measurements.

R: it appeared in the 'data acquisition method' of velmap project. Here, we also used the terminology. The electronic distance is a surveying and mapping technique.

19. Q: L133. Images with time span of 16 days to 3 years are used. What about the seasonal velocity variations? Can they be neglected?

R: Here, we use the time span to obtain the final mosaics of ice velocity. In mosaicking, the seasonal changes are not considered, the results can be considered to the average values over three years. But according to your advices, we now also provide the individual season products.

20. Q: L139. Coregistration and correlation are not synonym. They are two successive steps to generate accurate displacements.

R:Yes, the cross-correlation is one of methods to tackle with image registration problem. We used cross-correlation to stand for the registration in same manner as in the paper of Leprince et al. (2017). According to your advice, we now use 'coregistration' in introduction of method and the term 'correlation' is used in description of the techniques. 'or cross-correlation' is removed. thanks.

21. Q: L152. This is a complete mis-understanding of what cosi corr is doing. The coregistration is the step to obtain two images without any shift on the stable terrain (if stable terrain exist in the images). This is not the result of the first, coarse correlation. It gives the impression that the authors did not understand the tool that they have been using. Worrysome.

R: Please see above. The description about the coregistration of COSI-CORR was directly cited from the cosi-Corr guide in page 27. In my opinion, displacement can be obtained from the georeferenced images through two-step correlation under the geographic coordinate system. So, the first correlation for pixelwise displacement is called as coarse correlation and the second one for subpixel displacement can be viewed as fine correlation. The terms 'coarse or fine correlation' are from the InSAR coregistration.

22. Q: L159. 32 pixels means 480 m for the smaller correlation window. With such a window, does it make sense to generate a final map with a sampling distance of 100m? Authors should quantify what is the actual/true resolution of their dataset and use a relevant final grid size. Ground sampling distance and horizontal resolution are two different concepts.

R: In COSI-CORR, the sampling distance is controlled by step size not by Window Size. Here, we used the 7 pixels as step size and produced nearly 100m ground grids. As an illustration, we can produce higher resolution displacements as shown in Figure R1. The glacier is apparently less than 300m in width, but we still produce high resolution displacements as shown in right part of Figure R1.

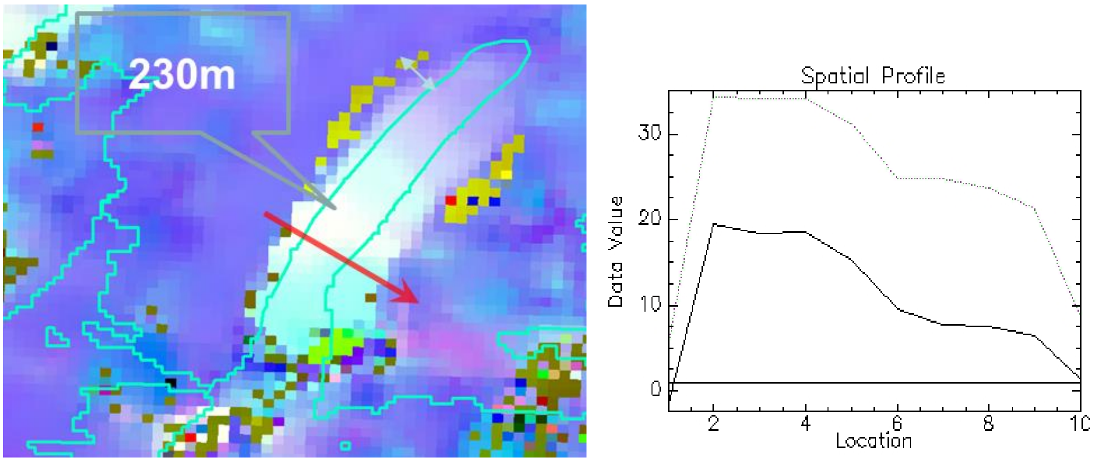

Figure R1. A sample of small glacier (left: glacier inventory, and ice velocity as background; Right: The profiles of ice velocity corresponding to the locations marked by red arrow on the left, thick line - WE velocity, thin line – NS velocity)

23. Q:. L179. Unclear how the QA band has been generated.

R: The downloaded packaged file of Landsat 8 includes the QA band. But information about cloud cover is coded in the band, we extracted the cloud coverage information using a procedure we developed. The QA band has been introduced in L179-187 in the original manuscript.

24. Q: L188. This is too vague. Which value are exactly excluded?

R: The edges of the displacement vector (image) are clipped in the process of mosaicking. For more clearly, we re-edit the sentence as follows, "the edges of the displacement vectors are masked in the process of mosaicking".

25. L201. This is this geolocation error that the coregistration aim at reducing. I understand it is difficult (or impossible) in Antarctica due to a lack of stable terrain (few nunataks). But I write this to make sure the authors understand what the coregistration step is

R. Agree. We understand the aim of coregistration step. Thanks.

26. Q: L211. How can the authors be sure that the INSAR dataset provide a good reference for slow moving areas? I noted many artefacts in the low velocity zone of Antarctica in the INSAR dataset.

R: In preparation of the manuscript, the published ice velocity is only InSAR dataset. We first used rock data and then used InSAR dataset, and only offset of differences between two datasets are applied in mosaicking. We selected InSAR velocity less than 10 m/yr as stagnant, which is generally under the uncertainty of satellite-derived ice velocity. Not only that, but we investigated their performances by comparing with in-situ measurements. furthermore, in revised manuscript, the gardner's ice velocity dataset is also included in assessment of the accuracy, the details can be found in main text.

27. Q: L232. Does it mean that more weight is given to the velocity measurements over longer time periods? Authors should be more explicit about that.

R: Yes, the equation 1 can be rewritten in the following for better clarity,

$$v = \frac{\triangle t_1 * \frac{\triangle d_1}{\triangle t_1} + \triangle t_2 * \frac{\triangle d_2}{\triangle t_2} + \cdots + \triangle t_n * \frac{\triangle d_n}{\triangle t_n}}{\triangle t_1 + \triangle t_2 + \cdots + \triangle t_n}$$

However, for the concise expression the equation still keeps unchanged.

28. Q: L247. Your ground sampling distance is finer. Authors did not demonstrate that the actual resolution of their product if finer. To be demonstrated. Authors need to show side by side their dataset with the Rignot & Gardner dataset to really illustrate their high resolution.

R: Our high-resolution results are shown in Figure 2 c as an illustration. Here we show the resolution comparisons of three groups of results (from our L8, InSAR and LISA) in Figure R2. In general, there are large fluctuation in velocity in high shear zone, both our result and LISA data can capture the velocity variations along profiles, but InSAR data do not capture any velocity changes. It can be easily seen that our result shows finer resolution.

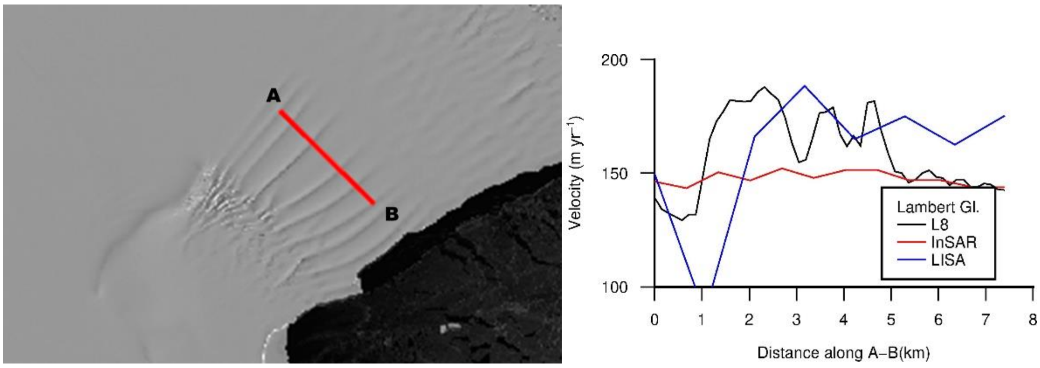

Figure R2. An illustration of A-B velocity profiles of three datasets(left: geolocation, right: the results)

29. Q: L255. Clarify that "fast ice" is on sea ice. Not obvious to all readers.

R: Fast ice that is anchored to the shore or ocean bottom, typically over shallow ocean shelves at continental margins; fast ice is defined by the fact that it does not move with the winds or currents. (ref. https://nsidc.org/cryosphere/glossary/term/fast-ice). Some explanation now is added in the text Line 20 in revised manuscript.

30. Q: L297. What does "predominant" mean? No really scientific Table 1. Why providing the "year" if it is always 2015...

R: We attempted to provide the time-stamped information for the products although there is multiyear combination. Here, we change the naming convention for the multiyear products and individual summer's ones. We refer the naming convention of Gardner's products, the file name will include the begin and end dates of images used.

31. Q: L315. Why is the validation called "technical"?

R: The term was cited from the other paper published. For less misleading, we change the term to 'Validation'

32. Q L317-321 example of sentences with redundant (or incoherent information).

R: Thanks. L317-319 have been deleted.

33. Q: L332. Here the initial definition of co-registration is correct. Not earlier in the text. However, decorrelation is not leading to bad coregistration. Again the authors seem to not understand the meaning of this word

R: Thanks. Here the decorrelation represents incorrect registration results, which was cited from InSAR coregistration field.

34. Q: L342. Authors are quoting a correlation error here, not a coregistration error

R: ok, for consistence, we change to correlation error. The argument has also been responded in Q20

35. Q: L350. This is true only if the velocity is not changing with time. How can the authors be sure?

R: The results can be considered to the average values over three years.

36. Q: L362. Constance of the coregistration error with space and time need to be demonstrated or backed up using a formula.

R: It is generally accepted since the coregistration /or correlation error (you used) is difficult to determine on pixel-by-pixel. For example, the 1/128 pixel in InSAR-derived datasets, we referred the Leprince's paper and considered the 1/10 pixel as the error (a more conservative estimate) .

37. Q: L383. This variability of glacier flow is excatly why their mosaicking strategy (three summer) is not appropriate

R: The product only gave the averaged glacier flow between 2014 to 2016. According to your advice, we now also provide the three each summer mosaics of ice velocity.

38. Q: L385. Is there a year for the Raup & Scambos référence?

R: Thanks, we now use a full citation information about the dataset according the ESSD requirements.

39. Q:L399. What about the Gardner et al. product? How does it compare to the same data points?

R: ok, our results are also compared with LISA product provided by Gardner et al (2018) and the results are shown in figure 5c. The statistical information has been shown in main text.

40. Q: L420. Why not a direct 1:1 comparison between the INSAR and L8 dataset (also in area flowing between 10 and 100 m/yr)?

R: We can find that the differences between satellite-derived ice velocity and in-situ measurements is predominately limited to $\pm$20m (Figure 6). We now also compare our L8 results with InSAR and LISA in the region with ice velocity of less than 20m/yr. Good agreements are shown in Figure R3.

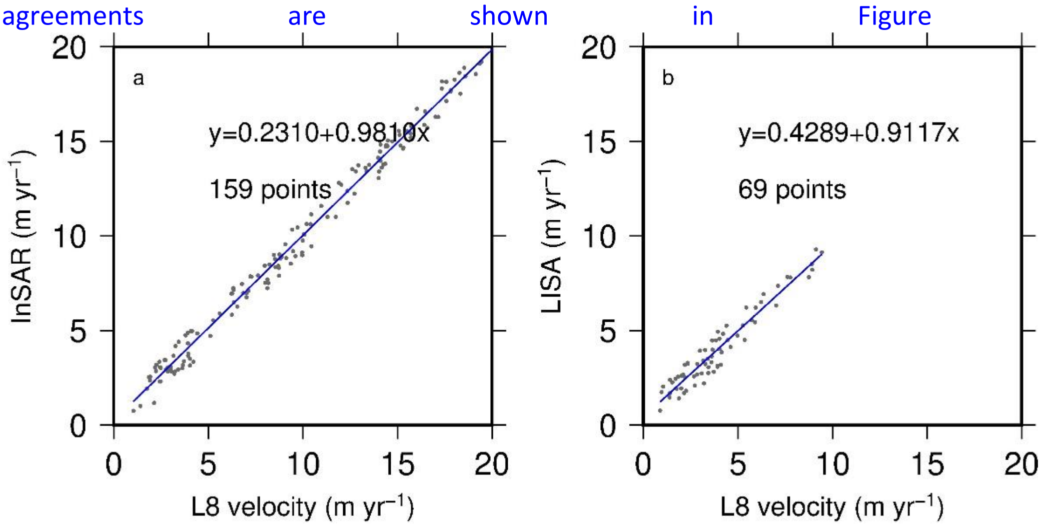

Figure R3 Our L8 results compared with InSAR and LISA datasets.

41. Q: L426. Validation on fast flowing glaciers, using data acquired 30 years ago in areas which are known to potentially experience profound change in velocity is not appropriate. I think it would be more convincing to construct two or three annual velocity maps and compare them. Over one year the assumption of little velocity change has more chance to hold. It would a useful check of internal consistency.

R: Although there is not appropriate, the analysis results shown the good consistence in velocity. In fast flowing region, some velocity profiles have been plotted and give the differences, which have been shown in figure 3. Here, we slight change the strategy of the analysis. The sites where ice velocity is larger than 400m yr^{-1} have been selected for the comparison. In addition, in order to reduce the possible impact of velocity change, we only investigated the sites where differences between satellite-derived ice velocity and in situ measurements are less than 50 m yr^{-1} in magnitude. Furthermore, we also provide the one-year products same as Gardner and Mouginot/Rignot do, and give a new paragraph and figure for description of internal consistency of annual ice velocity products. In whole processing, the LISA ice velocity is also included for the comparison.

~~Present-day~~ H~~h~~igh-resolution ice velocity data ~~map~~ of the Antarctic ice sheet from Landsat 8

Qiang Shen[1,3], Hansheng Wang[1,3], C. K. Shum[2,1], Liming Jiang[1,3], Hou Tse Hsu[1,3], Jinglong Dong[1,3], Song Mao[1,3], Fan Gao[1,3]

1. State Key Laboratory of Geodesy and Earth's Dynamics, Institute of Geodesy and Geophysics, Chinese Academy of Sciences, Wuhan 430077, China

2. Division of Geodetic Science, School of Earth Sciences, The Ohio State University, Columbus, Ohio 43210, USA

3. University of Chinese Academy of Sciences, Beijing 100049, China

Correspondence to: Qiang Shen (cl980606@whigg.ac.cn)

Abstract~~:~~

. Ice velocity constitutes a key parameter for estimating ice-sheet discharge rates and is crucial for improving coupled models of the Antarctic ice sheet to accurately predict its future fate and contribution to sea-level change. Here, we present new ~~a new~~ Antarctic ice velocity ~~map~~ maps at a 100-m grid spacing inferred from Landsat 8 imagery data collected from December 2013 through March 2016 and robustly processed using the feature tracking method. These maps were assembled from over 73,000 displacement vector scenes inferred from over 32,800 optical images. Our maps cover nearly all the ice shelves, f~~landf~~ast ice (anchored to the shore or ocean bottom), ice streams, and most of the ice sheet. The maps have an estimated uncertainty of less than 10 m yr^{-1} based on ~~robust~~ internal and external validations. These datasets will allow for a comprehensive continent-wide investigation of ice dynamics and mass balance combined with the existing and future ice velocity measurements and provide researchers access to better information for monitoring local changes in ~~ice~~ glaciers. Other uses of these datasets include control and calibration of ice-sheet modelling, developments in our understanding of Antarctic ice-sheet evolution, and improvements in the fidelity of projects investigating sea-level rise. All data presented here can be downloaded from the Data Publisher for Earth & Environmental Science (https://doi.pangaea.de/10.1594/PANGAEA.895738).

1 Introduction

Global warming could lead to significant mass changes in the Antarctic ice sheet. The ice mass of this sheet has a displacement potential equivalent to a sea level rise greater than 60-m (Fretwell et al., 2012;Alley et al., 2005), which would alter oceanic conditions and marine ecosystems, such as ocean currents, water temperature, and fishing ground distributions (Gutt et al., 2011). Monitoring the glacial dynamics of the ice sheet is a primary scientific goal to determine whether the ice sheet is stable, growing or shrinking. Thorough and continued monitoring of ice-sheet dynamics is also of utmost importance for accurate predictions of ice-sheet behaviour in the future (Joughin and Alley, 2011;van Wessem et al., 2016). Ice velocity, which is one key parameter representing ice dynamics, affects the estimates of ice-sheet mass balance and the corresponding sea level rise (Scheuchl et al., 2012) and plays a crucial role in studies on glacier dynamics and mass balance. The ice velocity of peripheral outlet glaciers is also one of the primary parameters needed to determine the ice discharge rate, because these glaciers act as channels for ice transportation from the ice-sheet interior to the ice shelves and ocean. A comprehensive and lasting observation of ice velocity is important to better understand a wide range of processes related to glacial mass fluxes, such as glacier response to climate and climatic changes, glacier physics and flow modes, glacier flow instabilities (e.g., surges), subglacial processes (e.g., erosion), and supra- and intra-glacial mass transport.~~Long-term and continuous measurements of ice velocity are a precondition for developing a complete understanding of the ice dynamics of the continent of Antarctica.~~ Furthermore, ice velocity products with a higher resolution can facilitate more thorough investigations on localized ice dynamics (Nath and Vaughan, 2003;Favier and Pattyn, 2015), such as the production of crevasses and the role of ice rises on ice sheet stability. These factors highlight the need for a new set of high-resolution ice velocity observations over Antarctica.

Ice velocity has been measured by traditional ground-based measurement techniques (e.g., GPS, electronic distance, aerial photograph) since the 1970s in the Antarctic ice sheet (Manson et al., 2000;Zhang et al., 2008;Kiernan, 2001;Rott et al., 1998). However, obtaining a complete real-time survey is ~~difficult~~ almost impossible due to the remoteness of the continent and extremely cold climate. Moreover, the sporadic and discontinuous measurements prohibit the study of ice-sheet mass balance as a whole (Bindschadler and Scambos, 1991;Scambos et al., 1992;Scheuchl et al., 2012). Recently, glaciologists have begun to present a complete picture of the ice velocity in Antarctica by using multi-satellite interferometric synthetic aperture radar (InSAR) at a 450-m spatial resolution (Rignot et al., 2011). Additionally, an updated dataset of annual InSAR-derived ice velocity was recently released at a 1000-m spatial resolution, and ~~another~~ continent-wide ice velocity maps from Landsat 8 (L8) images ~~was~~ were also reported ~~(Mouginot et al., 2017)~~ in a variety of spatial resolutions (~~300~~100-1000 m) (Mouginot et al., 2017;Gardner et al., 2018;Shen et al., 2018). ~~Long-term and continuous measurements of ice velocity are a precondition for developing a complete understanding of the ice dynamics of the continent of Antarctica. Furthermore, ice velocity products with a higher resolution can facilitate more thorough investigations on localized ice dynamics(Nath and Vaughan, 2003;Favier and Pattyn, 2015), such as the production of crevasses and the role of ice rises on ice sheet stability. These factors highlight the need for a new set of high-resolution ice velocity observations over Antarctica.~~

Deriving the surface velocity of glaciers and ice shelves using optical satellite images is a rapid, cost-effective method to obtain the large-scale ice velocity field, especially in remote Antarctica, which has been widely used in glaciology (Lucchitta and Ferguson, 1986;Bindschadler and Scambos, 1991;Scambos et al., 1992;Joughin et al., 2002;Scheuchl et al., 2012). However, the Antarctic-wide ice velocity based on optical satellite images remains difficult to determine, although relevant work has been performed since the mid-1980s. The near global coverage and high repeat rate of optical satellites now provides the possibility for continent-wide mapping and monitoring of glaciers and ice-sheet dynamics, especially the L8 mission. L8 is the ~~newest~~ most recent generation of satellites in the Landsat family and provides continuous coverage of earth’s surface with a 16-day revisit cycle at a 98.2 inclination. The Operational Land Imager (OLI) on L8 can provide improved radiometric and geodetic performance with a high spatial resolution (up to 15 m). The combination of a high repeat rate and good performance creates an opportunity to generate a continent-wide ice velocity map in Antarctica (Gardner et al., 2018).

Here, we present ~~a~~ high-resolution ice velocity mosaics of Antarctica (except for the area south of 82.5°S) inferred from L8 images from the United States Geological Survey (USGS) Earth Resources Observation and Science (EROS) Center, and annual mosaics of ice velocity are also ~~.~~available. These velocity data have the highest spatial resolution of 100 m achieved to date and were assembled from more than 73,000 scenes of displacement vectors. The vectors are inferred from more than 32,800 orthorectified panchromatic band scenes with a 15-m spatial resolution acquired by the OLI on L8 from December 2013 to March 2016 using the optical offset method (see Sect. 2). The flowchart for producing and validating the ice velocity data is shown in Figure 1. These newly generated datasets could be valuable in quantitative determination of ice discharge rates and mass balance of the Antarctic ice sheet at present and contribute to climatic modelling studies.

Section 2 presents detailed information on extracting the ice velocity, including an ice velocity generation method from displacement vectors and an error estimation approach. Section 3 presents the results and data records. Section 4 summarizes the accuracy validation process, including the technical validation and internal validation using independent data. The last section presents the conclusions.

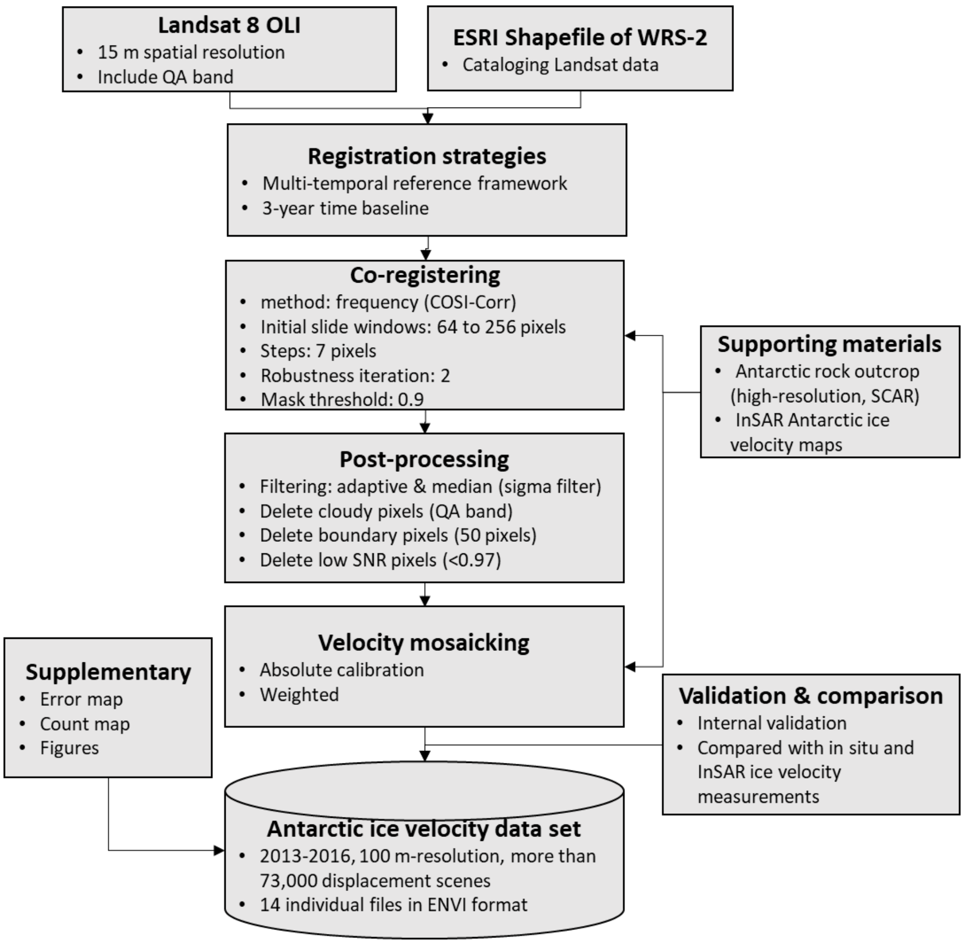

Figure 1. Flowchart for producing and validating the generated L8 Antarctic ice velocity dataset.

2 Data and methods

In this section, we first briefly present the satellite imagery data and existing ice velocity data collected using InSAR and field surveys (Sect. 2.1) and then summarize the pairing strategy of images (Sect. 2.2). Sections 2.3 to 2.5 summarize the feature tracking method of displacement, post-processing, ice velocity generation and mosaicking of Antarctic ice velocity maps.

2.1 L8 imagery data and other independent ice velocity measurements

In this study, the L8 orthorectified panchromatic band scenes are used to generate ice velocity maps ~~using the optical offset method, which will be summarized in Section 2.3.,~~. ~~and t~~The quality assessment (QA) band provides a cloud ratio to identify the spatial distributions of clouds and water, which are masked in displacement scenes. In addition, the supporting data contain the InSAR-derived Antarctic ice velocity data and LISA (Landsat 8 ice speed of Antarctica) (Scambos et al., 2019;Fahnestock et al., 2016), Antarctic rock outcrop data inferred from L8 (Burton-Johnson et al., 2016), and previous ice velocity measurements compiled and managed by the National Snow & Ice Data Center (NSIDC) and the Chinese Antarctic Center of Surveying and Mapping. Antarctic rock outcrop data and the InSAR-derived

Antarctic ice velocity data are used to identify the stagnant region for absolute calibration and to assess our maps. The existing measurements of ice velocity consist of satellite-derived measurements and in situ measurements, which total over 144,000 measurements. The data include more than 1100 in situ measurements from a variety of geodetic techniques, such as electronic distance, theodolites and GPS, and ~~electronic distance~~, which provide an external validation of our ice velocity maps.

2.2 Landsat 8 product and pairing strategy of images

The L8 Level 1 Systematic Terrain Corrected (L1GT) products in GeoTIFF file format were obtained from the USGS EROS Data Center (https://earthexplorer.usgs.gov/). The products consist of ten 30-m spectral bands with coverage of visible, near infrared, and shortwave infrared bands, a 15-m panchromatic band, product-specific metadata and a QA file. Here, we only use the panchromatic band because of its high resolution, product-specific metadata and QA file. More than 32,800 L1GT data have been processed to generate displacement vector scenes. To overcome the cloud contamination and improve the amount of measurements, we use the multiple reference strategy in image pairing, which means that all images in the same Worldwide Reference System (WRS-2) could be taken as reference images in the pairings. In addition, paired images are generated using a time interval of three years as a maximal temporal baseline with a minimum time separation of 16 days. Finally, more than 73,000 paired images are obtained to produce the surface displacement of the ice sheet.

2.3 Feature tracking processing

To determine the horizontal displacement vectors due to ice motion, we use a feature tracking method (Scambos et al., 1992;Bindschadler and Scambos, 1991;Leprince et al., 2007), also known as the phase-shift method. The orthorectified L8 images are directly used to produce the displacement vectors by means of the co-registration ~~(or cross-correlation)~~ method in the Co-registration of Optically Sensed Images and Correlation (COSI-Corr) software package developed at the California Institute of Technology (Leprince et al., 2007). Many studies have proven that this technique is more efficient for images under different illumination conditions (Heid and Kääb, 2012;Brown, 1992), especially in low visual contrast areas, such as Antarctica. The method produces displacement vectors by a phase-shift technique of low frequency calculated by a Fourier-based frequency correlator (Leprince et al., 2007), which is produced repetitively within a specific sliding window (or patch) on the paired images. The result is given by a three-band file consisting of an E-W displacement map (positive towards the east), an N-S displacement map (positive towards the north), and a signal-to-noise ratio (SNR) band as an indicator of the measurement quality. The technique can resolve sub-pixel displacements of less than 1/20 of the pixel resolution at a high SNR, which is generally greater than 0.9.

Specifically, the feature tracking processing has two stages. The first stage (namely, coarse ~~co-~~correlation~~registration~~) approximately estimates the pixelwise displacement between two patches. In general, if noisy images or large displacements are expected, a large initial sliding window should be used. In this study, the size of the initial sliding window varies from 64 to 256 pixels in both the X and Y directions according to a priori knowledge from the InSAR-derived Antarctic ice velocity and the time interval between two paired images. Once the initial displacements are estimated, the second stage consists of fine correlation~~co-registration~~ to retrieve the sub-pixel displacement using a smaller window. The new size of 32×32 pixels is tentatively adopted to yield reliable estimates for the displacement at densely independent points. Other parameters of the frequency correlator include the step sizes between sliding windows in both the X and Y directions (in pixels), the frequency masking threshold, the number of iterations for robustness, resampling and gridded output. The step size is set to a constant value of 7 pixels in each dimension or approximately a 100-m spatial resolution. A frequency masking threshold of 0.9 is adopted as the optimum value as recommended in a previous study (Leprince et al., 2007).

2.4 Post-processing displacement vectors

Generally, the frequency-based correlation ~~co-registration~~ method is more accurate than statistical methods but more sensitive to noise contamination. L8 images can minimize the effect because of the good radiometric and geodetic performances, but decorrelation still exists due to large ground motion, lack of measurable ground features (e.g., crevasses or rises), sensor noise, illumination conditions, atmospheric changes (e.g., clouds) and topographic artefacts (thereby producing imprecise orthorectified data). To overcome these problems, we devise three steps to enhance the signal and exclude unreliable measurements. First, we suppress the noise on each displacement scene using an adaptive filter and a median filter. The adaptive filter is the local sigma filter (Eliason and Mcewen, 1990) that features a filter size of 9 pixels and a sigma factor value of 2. A median filter is further applied to remove "salt and pepper" noise in ice displacement scenes. Second, the areas covered by clouds and water are excluded from the displacement scenes using the QA band (Zanter, 2016). In the QA band, each pixel contains a 16-bit integer that represents bit-packed combinations of surface, atmospheric, and sensor conditions at different confidence levels. The pixels covered by cloud and water in paired images are unpacked from the QA band using the procedures we have developed, and the pixels marked as clouds and water at high confidence levels (67–100%) are used to build a mask layer. These pixels are then masked in displacement scenes. Note that the identification of cirrus clouds is problematic in raw images based on our analysis, since radiometric characteristics of ice and cirrus clouds are generally indistinguishable. Here, we use only clouds to build a mask layer. Third, since frequency correlation easily causes errors at the edges of displacement scenes, the edges of the displacement vectors are masked in the process of mosaicking~~the results of the displacement vectors are neglected at the edge regions~~.

2.5 Ice velocity measurement

Cloud contamination is a major challenge in ice velocity estimation using optical images, which is particularly significant in polar regions (Toon and Turco, 1991). To overcome this problem, we process all image pairs using a time interval of three years as a temporal baseline with a minimum repeat cycle of 16 days in WRS-2. Some images in adjacent paths in the WRS-2 are also paired to determine the ice velocity for some void areas where no valid scenes with the same path and row are available. A three-year time interval is used in our processing. Although the decorrelation becomes more apparent with the increase in the time interval, many surface features on ice sheets remain preserved and visible over many years (Lucchitta and Ferguson, 1986). Finally, more than 73,000 image pairs are organized from more than 32,800 scenes of L8 panchromatic images and are processed to generate ice velocity estimates.

Despite the improved geometric accuracy of L8, the residual geolocation errors (~8 m circular error (90%)) of the L8 panchromatic band contribute most of the uncertainties in ice velocity products. These errors will lead to an offset between the displacement scenes and should be removed (Fahnestock et al., 2016). In fact, offset tuning is often called absolute calibration of the ice velocity data. In Antarctica, absolute calibration is a challenging issue because the ice is active almost everywhere and available rock outcrops are extremely scarce. Here, we use both rock outcrop data (Figure 3e) derived from L8 images(Burton-Johnson et al., 2016) and the InSAR-derived Antarctic velocity map(Mouginot et al., 2017) to determine the relatively stagnant areas (i.e., areas with InSAR-derived ice velocities of <10 m yr^{-1}) for the absolute calibration of our ice velocity estimates.

The velocity calibration consists of three steps. First, the differences in the displacements between the InSAR-derived velocity map and our calculated ice velocity maps from Landsat images are calculated in the stagnant areas. Second, to eliminate outliers, a 3σ filter is applied recursively on these differences. In this technique, the measurements of the differences are removed if the magnitudes of the values are larger than three times the standard deviation (3σ). Third, the mean of the remaining differences is considered the offset of the displacement scenes. Furthermore, the offsets for the displacement scenes outside of the stagnant areas (such as in the Ross and Ronne ice shelves) are estimated by overlapping neighbouring scenes captured at approximately the same time. The offsets of two velocity components are independently estimated. In addition, to be computationally efficient, Antarctica is divided into 16 gridded sub-regions, which are shown in Figure 2a, and data stacking is processed independently. Finally, the 14 sub-regions are mosaicked to generate an ice velocity map for all of Antarctica because two sub-regions do not cover the grounded ice sheet.

The mosaicked velocity maps are produced based on the displacement scenes. To increase the accuracy of the mosaicked velocity maps, we stack all displacement scenes after removing the pixels with an SNR less than 0.95. In general, the velocity map contains dozens of scenes in each location. For a specific pixel denoted by *i*, all displacement scenes (*m*=1, 2, …, *n*) are stacked to obtain the estimate of the ice velocity (V_i) as follows:

$$V_i = \frac{\sum_{m=1}^{n} \Delta d_m^i}{\sum_{m=1}^{n} \Delta t_m^i} \tag{1}$$

where Δd_m^i denotes the generated displacement during the time interval Δt_m^i.

3 Results

3.1 Antarctic-wide ice velocity map

Over Antarctica, valuable L8 images are available for only the summer and fall seasons, i.e., in November, December, January, February and March, which means that the L8 ice velocities represent mainly the summer/fall ice velocity. In Figure 2a, we show a mosaicked Antarctic ice velocity map inferred from over 73,000 L8 images acquired from December 2013 to March 2016. Our maps cover nearly all of the ice shelves, ice streams, and the majority of the ice sheet. Here, we undertook an improved post-processing method based on more paired displacement vectors in the generation of the new and improved Antarctica-wide ice velocity data products in comparison with our previous annual ice velocity data (Shen et al., 2018). ~~Here,~~ Figure 2b shows a count map to indicate the number of images used to produce the ice velocity data. ~~The predominant year of the images is 2015 (Figure 2b), and t~~There are generally more than 20 displacement vectors, with up to 200 in some regions. The L8 ice velocity map shows the same pattern as the InSAR-derived and LISA ice velocity map, and Figure 3 shows some ice velocity and the difference graphs from the three ~~two~~ ice velocity products. The spatial resolution of the L8 ice velocity data is 3 to 10 times finer or higher resolution than that of the recent L8-derived

(Gardner et al., 2018) and InSAR-derived ice flow maps (Mouginot et al., 2017;Rignot et al., 2011), reaching up to 100 m. Here, we show the velocity map of James Ross Island in the Antarctic Peninsula as an illustration of our high-resolution results (Figures 2c and 2d). The results reveal that the L8 velocity map can provide details of the ice velocity pattern for the Antarctic ice sheet, such as for James Ross Island and small glaciers (Figures 2c and 2d). Thus, our ice velocity map provides the first opportunity to investigate localized ice dynamics, such as crevasse formation, and the roles of ice rises and rumples in ice-sheet dynamics and evolution. These maps also have good coverage over Antarctica, except for south of 82.5°S. The mosaicked ice velocity map covers the majority of the Antarctic ice sheet and nearly 99% of the fast-flowing glaciers and ice shelves, as well as fast ice, except for a few ice streams located on the Ronne Ice Shelf (e.g., Academy and Foundation Glaciers) and on the Ross Ice Shelf (e.g., Whillans Glacier in the Siple Coast).

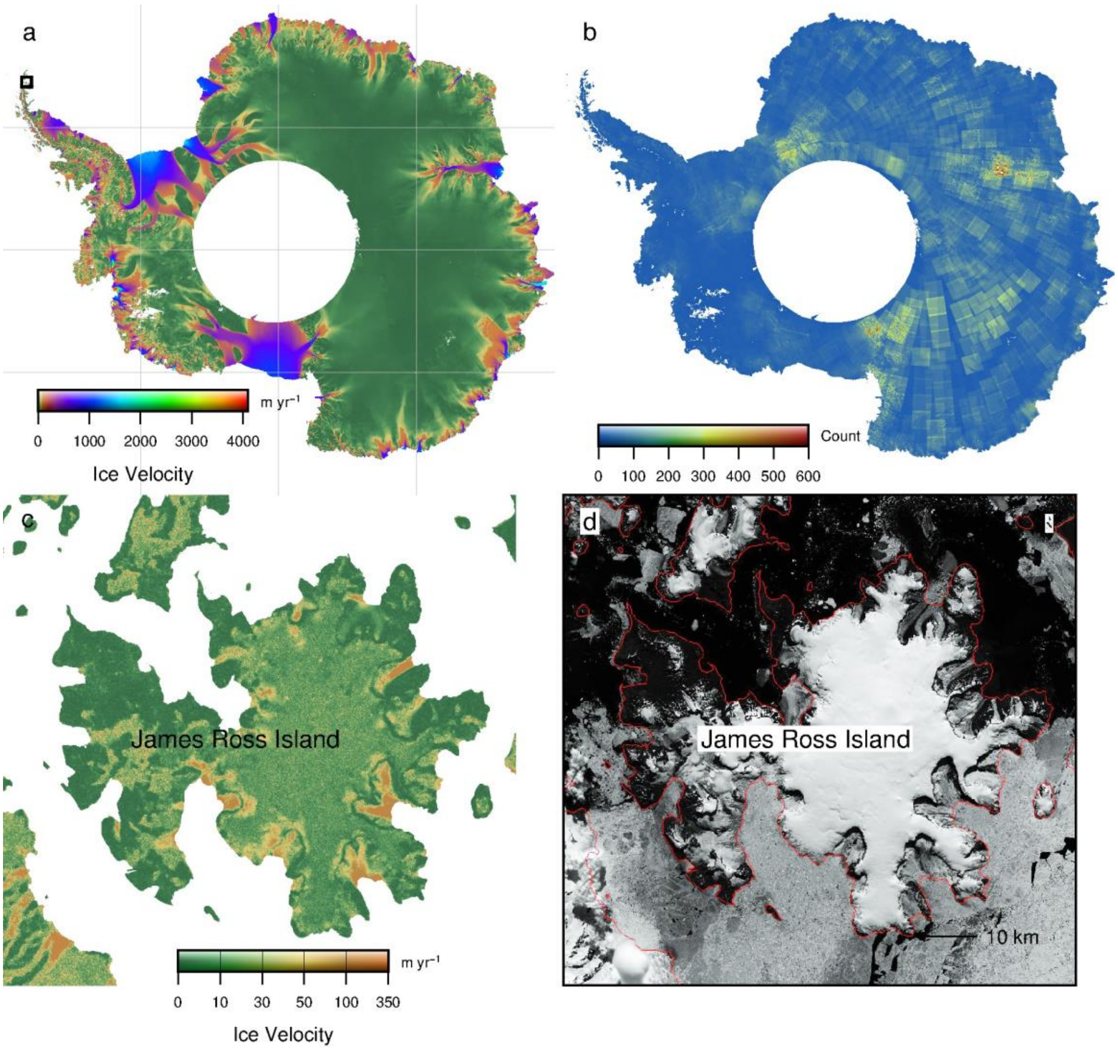

Figure 2. L8~~-derived~~ ice velocity data ~~estimates~~ from Landsat 8 images from December 2013 to March 2016. (a) L8-derived Antarctic ice velocity map (gridded lines delineate the 16 sub-regions); **(b)**

footprint map of L8 presenting the number of valid displacement vectors used to produce the ice velocity map in a specific grid (pixel); **(c)** magnified view of the ice velocity map of James Ross Island, Antarctic Peninsula, corresponding to the box in Figure 2a; and **(d)** L8 image corresponding to Figure 2c, in which the red solid line shows the coastal lines. The L8-derived ice velocity maps are drawn on a 500-m grid. The maps were created using The Generic Mapping Tools (http://gmt.soest.hawaii.edu/), Version 5.2.1.(Wessel et al., 2013)

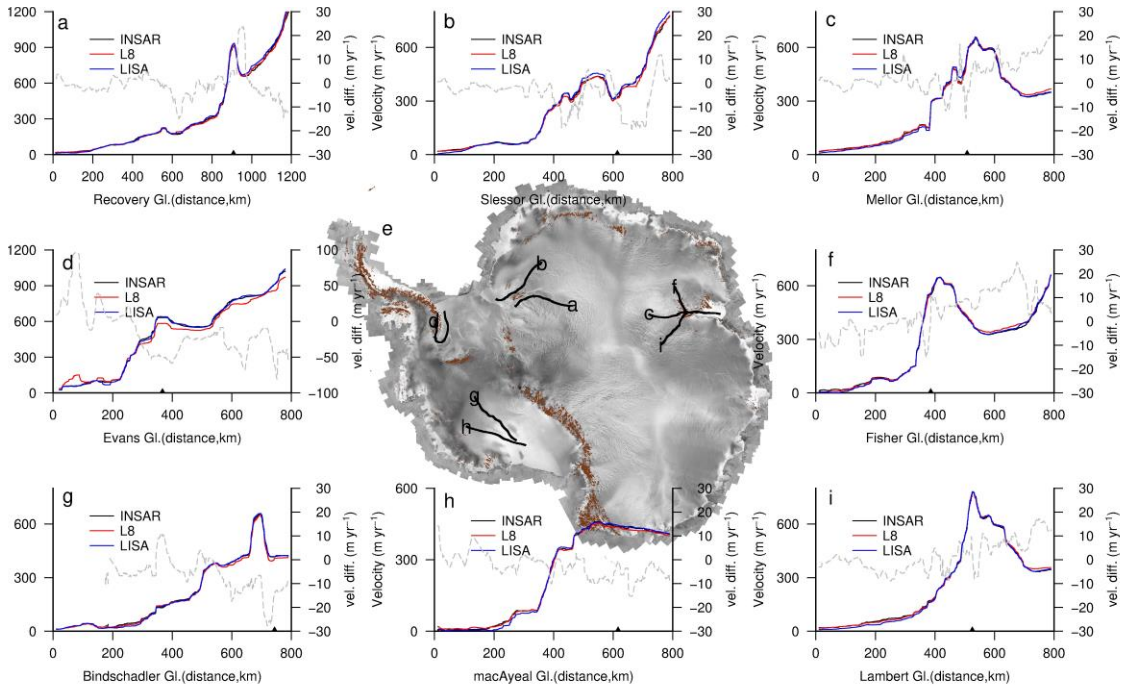

Figure 3. Velocity profile and the difference graphs comparing the L8 ~~(2015),~~ ~~and~~ InSAR and LISA ~~(2008)~~ ice velocity data. (**a**) Recovery Glacier; (**b**) Slessor Glacier; (**c**) Mellor Glacier; (**d**) Evans Glacier; (**e**) AMM RAMP Antarctic mosaic(Jezek and Team, 2002), in which the brown area shows the areas covered by rock outcrop. The black solid lines and the letters show the geolocations of the velocity profiles in a-i; (**f**) Fisher Glacier; (**g**) Bindschadler Glacier; (**h**) MacAyeal Glacier; and (**i**) Lambert Glacier. Left y-labels represent velocity magnitudes of glaciers, and the right y-labels are the differences of velocity magnitudes (L8-InSAR) along sampling paths shown in figure **e**. Black triangles represent the location of grounding lines. The maps were created using The Generic Mapping Tools (http://gmt.soest.hawaii.edu/), Version 5.2.1. (Wessel et al., 2013)

3.2 Data Records

The ice velocity map and supporting data are archived at https://doi.pangaea.de/10.1594/PANGAEA.895738. The ice velocity and footprints are made available in GeoTiff file format, Examples of the data products are shown in Figure 2.

3.2.1 Ice velocity map and error map

The 100×100-m gridded ice velocities for all of Antarctica are stored in a 16-bit long point GeoTIFF file format under a polar stereographic projection with a true latitude of 71°S. The gridded ice velocity has been equally divided into 4 subsets in the X and Y directions in consideration of file size and computer processing speed (Table 1). Note that file sizes have been kept to approximately 1 Gigabyte for user friendliness and easy downloading. Each file contains three bands that show velocity vectors in both the X-direction and Y-direction and a gridded error map of the ice velocity. The structure of the ice velocity filenames is Velocity_l8_*begin date*_*end date*_*subset*_*XY*_v1.tif, where Velocity represents ice velocity data and l8 indicates the L8 satellite from which images are used to produce the ice velocity map. * begin date * is start date of the images that contributed to mosaic in format of ‘yyyyddd’, which ‘yyyy’ is four-digit start year and ‘ddd’ is three-digit day of start year, and *end date* is end date of images used in same format with start date. *subset* shows whether the ice velocity file has been cropped due to considerations of file size and computer processing speed, and *XY* indicates the relative coordinates among all files, where X is the column number starting with one and Y is the row number starting with one. Furthermore, the ~~one-year~~annual mosaics of ice velocity are also provided. the ~~.~~ ~~N~~naming convention is the same as the description mentioned above.

Table 1. Filename structure of the ice velocity files. Two tiles do not include any valid ice velocity values.

Ice velocity filenames	column	row	subset
Velocity_l8_2013~~10~~33~~2~~6_~~2016360~~2016078_1_11_v1.tif	1	1	1
Velocity_l8_2013336_2016078~~2013102_2016360~~_2_12_v1.tif	2	1	2
Velocity_l8_2013336_2016078~~2013102_2016360~~_3_13_v1.tif	3	1	3

Velocity_l8_2013336_2016078~~2013102_2016360~~_4_14_v1.tif	4	1	4
Velocity_l8_2013336_2016078~~2013102_2016360~~_5_21_v1.tif	1	2	5
Velocity_l8_2013336_2016078~~2013102_2016360~~_6_22_v1.tif	2	2	6
Velocity_l8_2013336_2016078~~2013102_2016360~~_7_23_v1.tif	3	2	7
Velocity_l8_2013336_2016078~~2013102_2016360~~_8_24_v1.tif	4	2	8
Velocity_l8_2013336_2016078~~2013102_2016360~~_9_31_v1.tif	1	3	9
Velocity_l8_2013336_2016078~~2013102_2016360~~_10_32_v1.tif	2	3	10
Velocity_l8_2013336_2016078~~2013102_2016360~~_11_33_v1.tif	3	3	11
Velocity_l8_2013336_2016078~~2013102_2016360~~_12_34_v1.tif	4	3	12
Velocity_l8_2013336_2016078_13_41_v1.tif	Not provided. Subset does not cover the grounded ice sheet.		
Velocity_l8_2013336_2016078_14_42_v1.tif			
~~Velocity_l8_2013102_2016360_13_41_v1.tif~~			
~~Velocity_l8_2013102_2016360_14_42_v1.tif~~			
Velocity_l8_2013336_2016078~~2013102_2016360~~_15_43_v1.tif	3	4	15
Velocity_l8_2013336_2016078~~2013102_2016360~~_16_44_v1.tif	4	4	16

3.2.2 Landsat ground footprints

Landsat gridded footprints are stored in 8-bit integer point GeoTIFF files (Figure 2b), which show the number of displacement vectors used to produce the ice velocity at a specific location. These files also have the same file structure and projection as the gridded ice velocity map. The naming convention of the footprint maps is Footprints_l8_*begin date*_*end date*_*subset*_*XY*.~~dat~~tif, which has the same naming convention as the ice velocity maps, except for "Footprints", which indicates the content of the product.

4 Validation

Here, we describe and assess the precision by internal validation and comparison with in situ measurements. For internal validation, we produce the gridded error maps for the velocity maps. Furthermore, we compared our velocity maps with the InSAR-derived and LISA ice velocity map and in situ measurements as well as pre-existing measurements from remote images using co-registration vectors.

4.1 Internal validation

In the absence of other synchronously independent measurements of ice velocity, the uncertainty in the ice velocity maps from empirical analysis is generally used as an estimate of the accuracy of the ice velocity product. The error sources of L8-derived ice velocity are primarily attributed to the following three aspects: image co-registration, paired image time interval, and stacked data quantity.

Image co-registration represents a process of geometrically aligning two or more satellite images to obtain the corresponding pixels or feature representing the same surface objects, which is a main factor that influences the ice velocity accuracy. The image co-registration accuracy is largely determined by the following three factors: (1) decorrelation due to dramatic ground changes and a lack of measurable features between the scenes due to long time intervals or low-contrast land cover (e.g., snow or ice); (2) low image quality caused by sensor noise, pixel oversaturation, aliasing and cloud contamination; and (3) topographic artefacts caused by shadowing differences and inaccurate orthorectification of satellite attitudes. In fact, quantifying the effects of the three error sources is very difficult, especially on a pixel-by-pixel scale. In general, the co-registration accuracy is given empirically based on the validation of the matching algorithm. Here, the correlation error is equal to 1/10 of the pixel size in the E-W and N-S displacement components. This value is greater than 1/50 of the pixel size proposed by Leprince *et al.* (2007)(Leprince et al., 2007).

The second factor is the time interval of the paired images, because ice velocity is a function of displacements and time. Ice velocity is calculated by the displacement divided by the time interval of paired images. The uncertainty of the displacement is primarily attributed to image co-registration as mentioned above. Thus, a longer time interval suggests higher precision of the ice velocity (see Eq. 2).

The third factor is the amount of stacking data. Hence, more displacement data are stacked and will be more accurate. As a result, the gridded error map of ice velocity data can be obtained pixel by pixel based on the method of error propagations using the co-registration accuracy, time interval and total amount of stacking data.

According to the mosaicking method discussed above (Eq. 1), the uncertainty in one mosaicked velocity component at the *i*-th pixel (denoted by σ_{V_i}) can be estimated using the following error propagation formula under the assumption that the errors from different sources are independent and any temporal errors are negligible:

$$\sigma_{\mathrm{V_i}} = \pm\sqrt{\sum_{m=1}^{n}(\sigma_{\mathrm{m}}^{\mathrm{i}})^2 / \left(\sum_{m=1}^{n}\Delta t_{\mathrm{m}}^{\mathrm{i}}\right)^2} \quad (2)$$

where $\sigma_{\mathrm{m}}^{\mathrm{i}}$ is the co-registration error, i.e., the standard deviation of the *m*-th displacement observation during the time interval $\Delta t_{\mathrm{m}}^{\mathrm{i}}$. Since the co-registration errors are constant in the spatial (the whole scene) and temporal domains (all stacked displacements), if $\sigma_{\mathrm{m}}^{\mathrm{i}}$ is assumed to be a constant of σ, Equation (2) can be simplified as follows:

$$\sigma_{\mathrm{V_i}} = \pm\sqrt{\mathrm{n}}\,\sigma / \sum_{m=1}^{n}\Delta t_{\mathrm{m}}^{\mathrm{i}} \quad (3)$$

Since the E-W and N-S components at the *i*-th pixel have the same uncertainty, which can be calculated with Equation (3), the uncertainty is valid for the magnitude of the velocity vector. The error map (Figure 4a) in the magnitude of the mosaicked velocity vector is generally better than 10 m yr^{-1}, except for some areas in the Antarctic Peninsula and Marie Byrd Land in West Antarctica. Fewer valid satellite images are obtained from the two regions due to heavy cloud coverage. Relatively large uncertainties in these areas were mainly caused by a small amount of valid displacement vectors. For comparison, the error map of the InSAR and LISA ice velocity estimates is shown in Figure 4b and 4c, which quantifies the achieved accuracy of the ice velocity maps of this study. It is noted that the LISA error map is directly computed from the ice-velocity error (m/day) based on the law of error propagation.

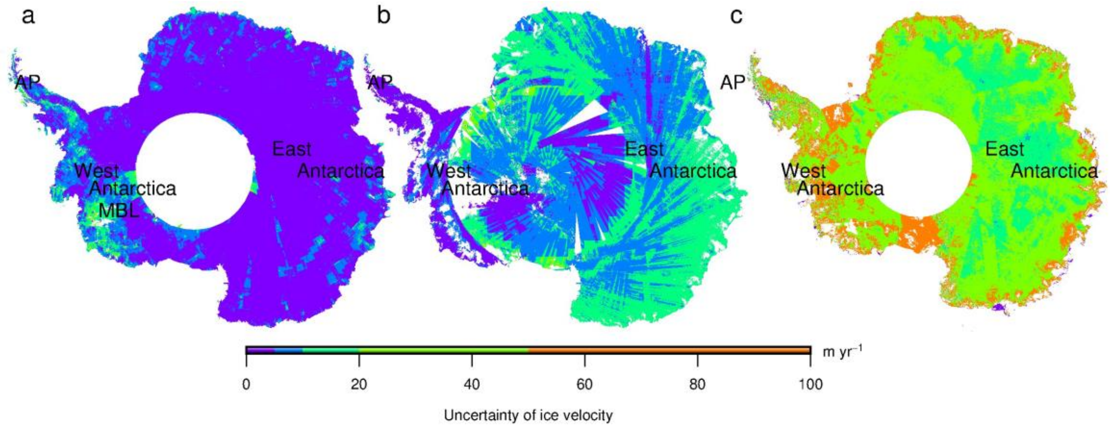

Figure 4. Uncertainty maps of the L8-derived Antarctic ice velocity (**a**), ~~and~~ InSAR-derived ice velocity(Mouginot et al., 2017) (**b**), and LISA ice velocity(Gardner et al., 2018) (**c**) MBL: Marie Byrd Land. The maps were created using The Generic Mapping Tools (GMT, http://gmt.soest.hawaii.edu/), Version 5.2.1.(Wessel et al., 2013)

4.2 Comparisons with other datasets and in situ measurements

A comparison of our velocity measurements with previous velocity measurements would be very beneficial. However, this comparison is very difficult due to the variability of glacier flow. Some glacier flow may vary significantly on daily, seasonal and yearly scales. Here, we collected historical long-term ice velocity measurements compiled and managed by the project of Velmap (Raup and Scambos, 2000) . Our ice velocity results are compared with only the in situ measurements located in the slow-flowing areas (<100 m yr^{-1}) because highly dynamic changes in ice velocity in fast-flowing areas (e.g., ice shelf) are expected. Furthermore, the ice velocity measurements on Byrd Glacier determined by photogrammetric methods and on Amery ice shelf from theodolite/EDM and GPS methods are used to illustrate the performance of our ice velocity map (Brecher, 1982;Brecher, 1986;Allison, 1979). A total of 609 sites in slow-flowing areas were chosen for comparison and analysis, and their differences are shown with dots in Figure 5a, where the colours of the dots denote the magnitude of the differences. Figure 5b shows the histogram of the differences between our velocity data and the in situ measurements. Except for three sites (two in Lambert-Amery Basin in East Antarctica and one on the Siple Coast in West Antarctica) (Figure 5a), the points are all less than 40 m yr^{-1}, and 593 sites, representing more than 97% of the total check points, have differences in the ice velocity magnitude of less than 10 m yr^{-1}. The differences have a –0.7 m yr^{-1} mean value and a 3.2 m yr^{-1} standard deviation. For comparison, the differences between the LISA ~~InSAR~~and InSAR velocity and field surveying data are shown in Figure 5c and 5d. For LISA dataset, a total of 469 points are less than 10 m yr^{-1}. These points have a mean value of -1.9 m yr^{-1} and a standard deviation of 4.5 m yr^{-1}, which shows slightly different pattern in which there is an apparent offset with in situ measurements. A total of 589 points are less than 10 m yr^{-1} ~~10 m yr^{-1}~~. These points have a mean value of 0.3 m yr^{-1} and a standard deviation of 3.3 m yr^{-1}. To further investigate the performance of the L8 ice velocity data in slow-flowing areas, we compared the L8, LISA, InSAR and in situ measurements with ice velocity magnitudes of less than 20 m yr^{-1}. The analysis results are shown in Figure 6. Figures 6a, ~~and~~ 6b and 6c show the relationships ~~difference~~ between the L8, InSAR and LISA ice velocity data and in situ measurements and the statistical results of these differences. The near-zero y-intercept and nearly unitary slope of the data in Figure 6a confirm that the L8 ice velocity data are very consistent with the in situ measurements, even in the stable interior ice sheet. Figure ~~6c~~ 6b shows the InSAR results and the similar performance with the L8 ice velocity data. However, for LISA, the data points are significantly smaller than the former two data (Figure 6c). In summary, the L8 ice velocity data have an accuracy of 10 m yr^{-1} (3σ).

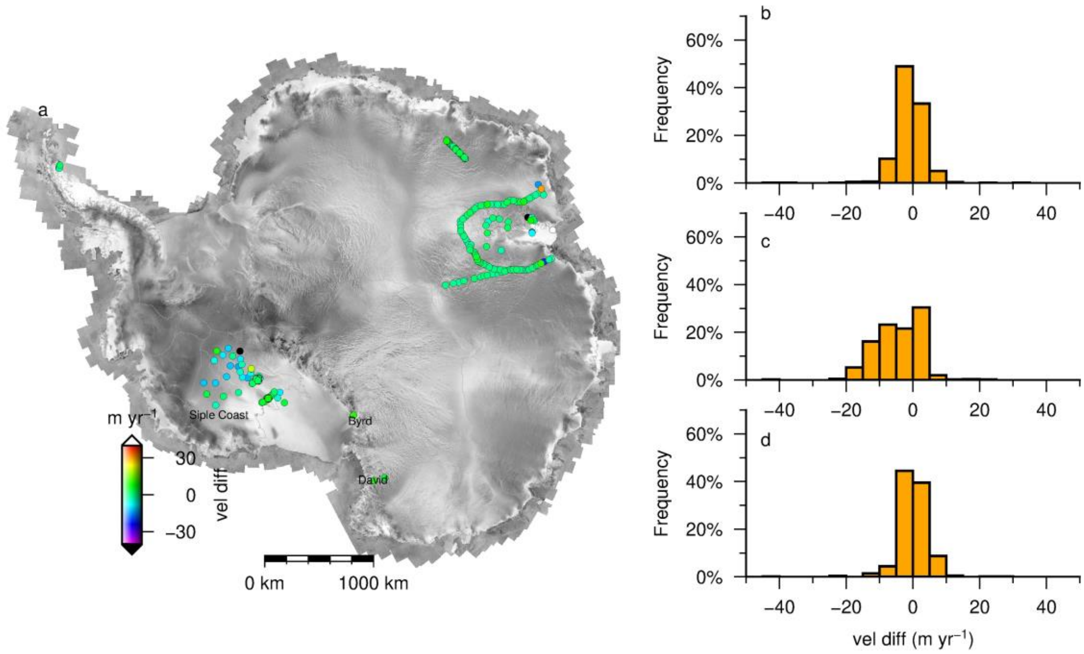

Figure 5. Accuracy assessment of L8 ice velocity and InSAR velocity. (**a**) Differences between in situ measurements and L8 ice velocity, where the colour dots show the geolocations and velocity differences between the L8 and in situ measurements (background maps are from the AMM RAMP Antarctic mosaic(Jezek and Team, 2002)); (**b**) histogram of the differences between the L8 and in situ ice velocity

data; ~~and~~ (**c**) histogram of the differences between the LISA ~~InSAR~~ and in situ ice velocity data; and (**d**) histogram of the differences between the InSAR and in situ ice velocity data.~~.~~

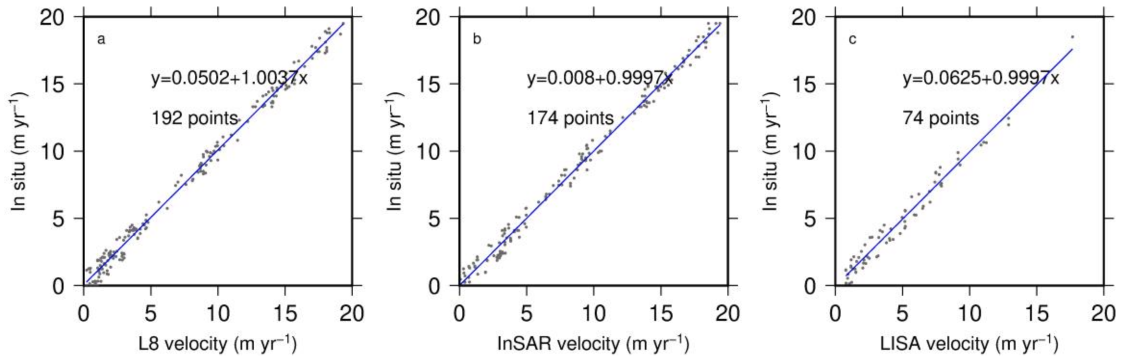

Figure 6. Comparison between the in situ measurements and L8 ice velocity (a), ~~and~~ InSAR (b) and LISA (c)

To assess the reliability of the L8 ice velocity data in fast-flowing areas, here, we show two illustrations of Byrd Glacier (80°S, 160°E) and Amery ice shelf (69°S, 71°E), which were thought to be relatively stable~~)~~. For Byrd Glacier, the in situ ice velocity measurements were determined by photogrammetric methods from two sets of aerial photographs acquired on 6 December 1978 and 21 January 1979 (Brecher, 1982). In total, ice velocities of 470 sites on the main ice stream were determined by the change in location of natural features over the 56-day interval between two flights. Here, we analysed ~~436~~ 363 sites where the velocity is greater than ~~100~~ 400 m yr^{-1}. In order to reduce the possible impact of velocity change, we only investigated those sites where the differences between satellite-derived ice velocity and in situ measurements are less than 50 m yr^{-1} in magnitude. The near unitary slope of Figure 7b shows that L8 and the aerial ice velocity data have a good correlation, except for a small number of sites that have a relatively large difference. Figure 7a shows that the sites with large differences are located mainly on the lateral side of the glacier (see red and dark blue dots in Figures 7a and 7b). The large difference may be caused by the following factors: (1) errors in the two datasets, (2) relatively low resolution of the L8 ice velocity relative to the aerial method and high-velocity gradient on the sides of the glacier, which easily causes large differences, and (3) velocity changes between the long time intervals. For comparison, we also show the InSAR, LISA and aerial ice velocity in Figure 7c and Figure 7d, which shows that the L8, ~~and~~ InSAR and LISA ice velocity in fast-flowing areas have the ~~same~~ similar performance ~~as those shown in Figures 7b and 7c~~. On Amery ice shelf, the in situ ice velocity measurements were determined by using a combination of standard surveying techniques, including electronic distance and theodolites and GPS. The ice velocity observations on Amery ice shelf were mainly collected during two time periods

(December 1968—January 1970; December 1988—January 1991). Finally, the ice velocity measurements of ~~120~~ 59 sites (>400 m yr^{-1} in velocity) were compared with the L8, ~~and~~ InSAR and LISA ice velocity data. The vast majority of differences are less than 200 m yr^{-1}, except for a ~~small numbers~~small number of sites beyond the range (Figure ~~7d~~7e). The sites with large differences are mainly located on the front of the ice shelf. The L8 ice velocity data agree well with the in situ measurements in Figure ~~7e~~7f in same process strategy for Byrd glacier. For comparison, the InSAR, LISA and in situ measurements are also shown in Figures ~~7f~~7g and 7h, which also shown good consistency. ~~. An increase in the ice velocity is observed between the two time periods along the lateral route at an average velocity of 800 m yr^{-1} (Figures 7d and 7e), and this phenomenon is also shown in Figure 7f. The apparent changes in ice velocities may suggest different patterns in the dynamic characteristics.~~

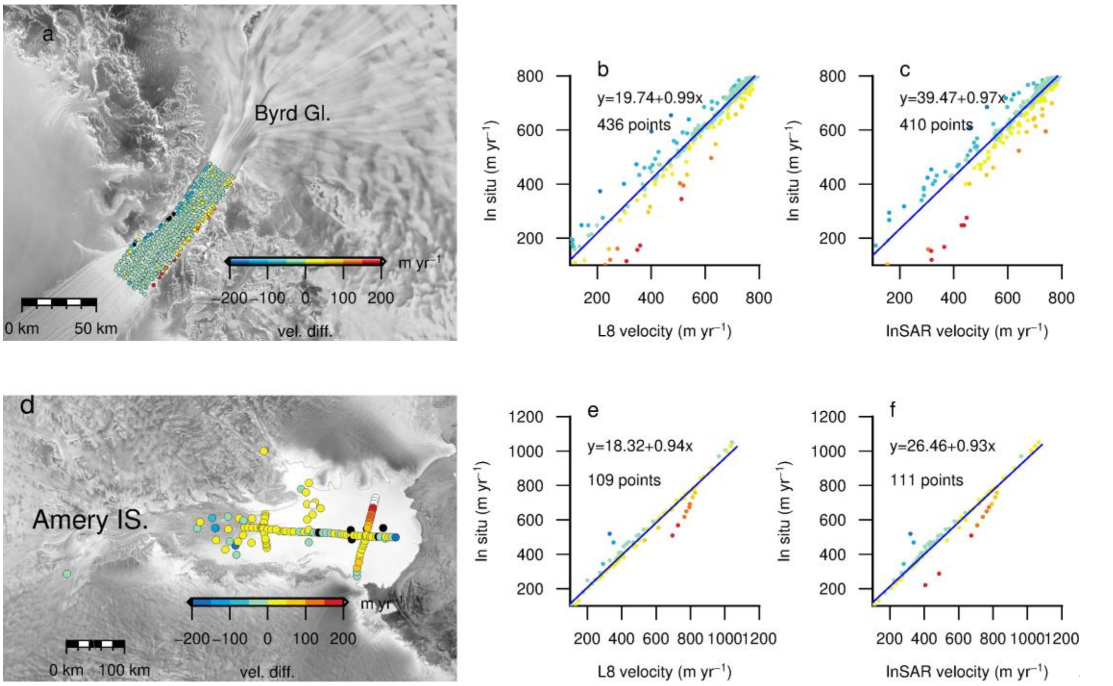

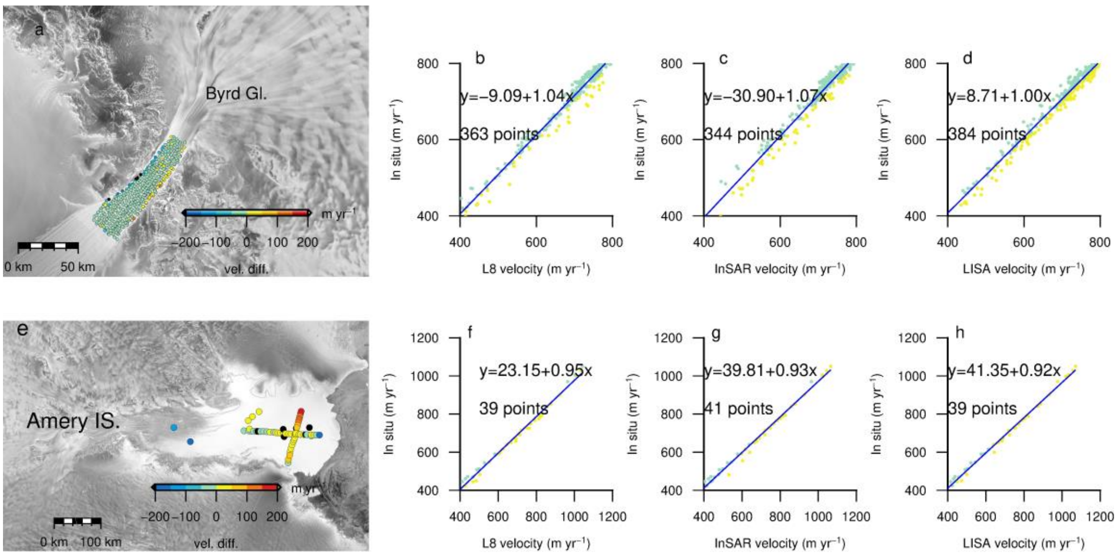

Figure 7. Comparison among the L8, InSAR and in situ measurements. (a) Byrd Glacier and the differences between the L8 and in situ ice velocity data (colour dots); note that the black dots represent differences of less than -200 m yr^{-1}, and the white dots represent differences of greater than 200 m yr^{-1}, (b) comparison between the L8 and in situ measurements on Byrd Glacier, (c) comparison between the InSAR and in situ measurements on Byrd Glacier, (d) comparison between the LISA and in situ measurements on Byrd Glacier; (~~d~~e) Amery ice shelf and the differences between the L8 and in situ ice velocity data (colour dots), (~~e~~f) comparison between the L8 and in situ measurements on Amery ice shelf, ~~and~~ (~~f~~g) comparison between the InSAR and in situ measurements on Amery ice shelf and (h) comparison between the LISA and in situ measurements on Amery ice shelf.

In addition, the annual Antarctica-wide ice velocity data products are also provided with full mosaics. In order to validate the accuracy including the internal consistency, we investigated the differences between the annual and the L8 mosaic ice velocity products. As an illustration, the profiles of ice velocities sampled on three glaciers (Lambert, Fisher, and Mellor glaciers) in the Lambert-Amery system, Antarctica, where there are predominately very little variations of ice velocity over the last decades. The investigations are implemented to calculate velocities along a long distance (more than 800 km) from the interior of the Antarctic Ice Sheet to the frontal parts of fast-flow Amery ice shelf (Figure 8). The variations of the magnitude of ice velocity show good internal consistency (less than 10 m yr^{-1}), even in the high stress zones, such as in the vicinity of grounding lines. An exception occurs in the front location of the Amery ice shelf, where it is thought to be exhibiting larger interannual variations in ice flows.

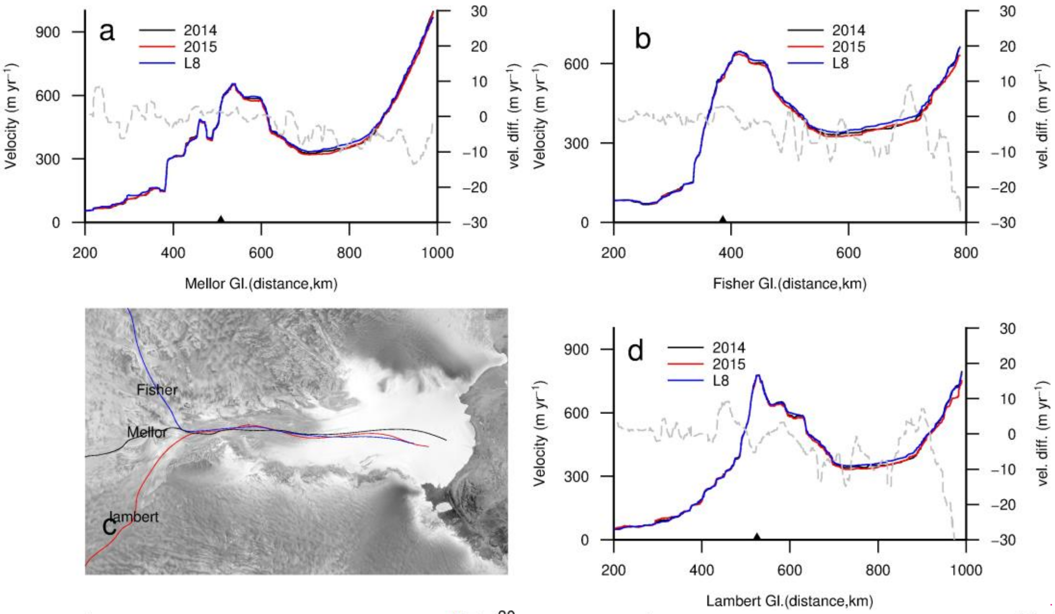

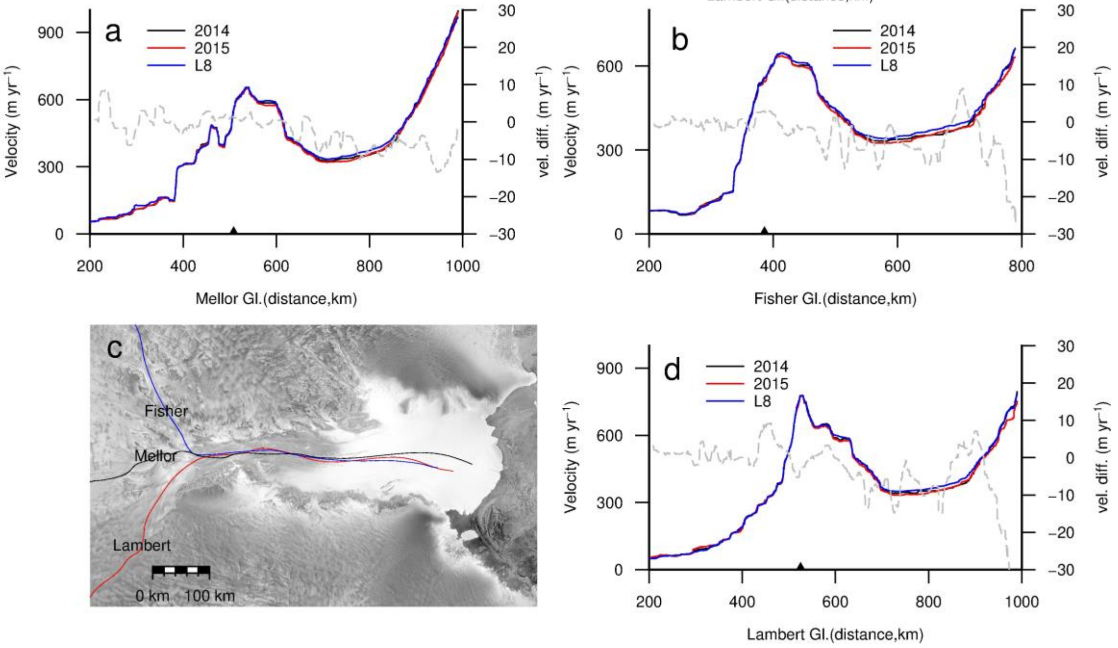

Figure 8. Example profiles of the L8 ice velocity products in Mellor (**a**), Fisher (**b**), and Lambert glaciers (**d**). The left vertical axes show the three glacier velocities (denoted by three color lines) along the profiles (**c**), and the right vertical axes are the differences of velocity magnitudes (2014–2015, dashed lines) along the profiles (**c**). Black triangles represent the location of grounding lines. The labels '2014' and '2015' are the annual ice velocity data and 'L8' is the full mosaic of ice velocity data. The maps were created using The Generic Mapping Tools (http://gmt.soest.hawaii.edu), Version 5.2.1 (Wessel et al., 2013).

5 Conclusions

Cold regions are very sensitive to the impacts of climate change. Long-term monitoring of ice-sheet dynamics is crucial for precise assessments of the glacial responses to climate change. We constructed a new Antarctic-wide high spatial resolution ice velocity map inferred from Landsat 8 imagery data collected between 2013 and 2016. The new map will provide an ~~opportunities~~opportunity to comprehensively investigate Antarctic ice dynamics in combination with existing and future ice velocity maps, which will provide insights into the ice sheet's mass balance.

Data availability

The latest dataset is available at the Data Publisher for Earth & Environmental Science (https://doi.pangaea.de/10.1594/PANGAEA.895738)

Author contributions

Q.S. conceived of, designed and conducted the experiment. H.W. contributed to the research framework and helped develop the methodology. C.K.S. and L.J. performed the data analysis. H.T.H. contributed to analysing the results. J.D., S.M. and F.G. contributed to the data processing. All authors contributed to the discussion and writing of the manuscript.

Competing interests

The authors declare that they have no competing interests.

Acknowledgements

We thank the National Aeronautics and Space Administration (NASA) and United States Geological Survey (USGS) for providing the Landsat-8 data. We thank E. Rignot and Alex S. Gardner at the Jet Propulsion Laboratory/California Institute of Technology for providing their ice velocity products. Financial support is provided by the National Key R & D Program of China (2017YFA0603103), the National Natural Science Foundation of China (Grant Nos. 41431070, 41590854 and 41621091), the Key Research Program of Frontier Sciences, CAS (Grant Nos. QYZDB-SSW-DQC027 and QYZDJ-SSW-DQC042), NASA (Grant No. NNX10AG31G), and the "Strategic Priority Research Program" of the Chinese Academy of Sciences(XDA19070302). We also appreciate the efforts of Amelie Driemel, the Data Publisher for Earth & Environmental Science, toward archiving the data at the World Data Center PANGAEA.

References

Alley, R. B., Clark, P. U., Huybrechts, P., and Joughin, I.: Ice-sheet and sea-level changes, Science, 310, 456-460, 2005.

Allison, I.: The mass budget of the Lambert Glacier drainage basin, Antarctica, J Glaciol, 22, 223-235, 1979.

Bindschadler, R. A., and Scambos, T. A.: Satellite-Image-Derived Velocity-Field of an Antarctic Ice Stream, Science, 252, 242-246, 1991.

Brecher, H.: Surface velocity determination on large polar glaciers by aerial photogrammetry, Ann. Glaciol, 8, 22-26, 1986.

Brecher, H. H.: Photogrammetric determination of surface velocities and elevations on Byrd glacier, 79-81 pp., 1982.

Brown, L. G.: A Survey of Image Registration Techniques, Comput Surv, 24, 325-376, 1992.

Burton-Johnson, A., Black, M., Fretwell, P. T., and Kaluza-Gilbert, J.: An automated methodology for differentiating rock from snow, clouds and sea in Antarctica from Landsat 8 imagery: a new rock outcrop map and area estimation for the entire Antarctic continent, The Cryosphere, 10, 1665-1677, 10.5194/tc-10-1665-2016, 2016.

Eliason, E. M., and Mcewen, A. S.: Adaptive Box Filters for Removal of Random Noise from Digital Images, Photogramm Eng Rem S, 56, 453-458, 1990.

Fahnestock, M., Scambos, T., Moon, T., Gardner, A., Haran, T., and Klinger, M.: Rapid large-area mapping of ice flow using Landsat 8, Remote Sensing of Environment, 185, 84-94, 2016.

Favier, L., and Pattyn, F.: Antarctic ice rise formation, evolution, and stability, Geophys. Res. Lett., 42, 4456-4463, 10.1002/2015gl064195, 2015.

Fretwell, P., Pritchard, H., Vaughan, D., Bamber, J., Barrand, N., Bell, R., Bianchi, C., Bingham, R., Blankenship, D., and Casassa, G.: Bedmap2: improved ice bed, surface and thickness datasets for Antarctica, The Cryosphere, 7, 375-393, 2012.

Gardner, A. S., Moholdt, G., Scambos, T., Fahnstock, M., Ligtenberg, S., van den Broeke, M., and Nilsson, J.: Increased West Antarctic and unchanged East Antarctic ice discharge over the last 7 years, The Cryosphere, 12, 521-547, 10.5194/tc-12-521-2018, 2018.

Gutt, J., Barratt, I., Domack, E., d'Udekem d'Acoz, C., Dimmler, W., Grémare, A., Heilmayer, O., Isla, E., Janussen, D., Jorgensen, E., Kock, K.-H., Lehnert, L., López-González, P., Langner, S., Linse, K., Manjón-Cabeza, M., Meissner, M., Montiel, A., Raes, M., and Smith, C.: Biodiversity change after climate-induced ice-shelf collapse in the Antarctic, 2011.

Heid, T., and Kääb, A.: Evaluation of existing image matching methods for deriving glacier surface displacements globally from optical satellite imagery, Remote Sensing of Environment, 118, 339-355, 2012.

Jezek, K., and Team, R. P.: RAMP AMM-1 SAR image mosaic of Antarctica, Digital media. Fairbanks, AK: Alaska Satellite Facility, and Boulder, CO: National Snow and Ice Data Center, 2002.

Joughin, I., Tulaczyk, S., Bindschadler, R., and Price, S. F.: Changes in West Antarctic ice stream velocities: Observation and analysis, J. Geophys. Res., 107, 2289-2289, 2002.

Joughin, I., and Alley, R. B.: Stability of the West Antarctic ice sheet in a warming world, Nature Geosci., 4, 506-513, 2011.

Kiernan, R.: Ice sheet surface velocities along the Lambert Glacier Basin traverse route, Research report (Antarctic CRC) ; no. 23., Accessed from https://nla.gov.au/nla.cat-vn1549959, edited by: Australia. Antarctic, D., and Antarctic, C. R. C., Antarctic CRC ; Australian Antarctic Division, Hobart, Tas, 2001.

Leprince, S., Barbot, S., Ayoub, F., and Avouac, J. P.: Automatic and Precise Orthorectification, Coregistration, and Subpixel Correlation of Satellite Images, Application to Ground Deformation Measurements, IEEE Transactions on Geoscience & Remote Sensing, 10, 1529-1558, 2007.

Lucchitta, B. K., and Ferguson, H. M.: Antarctica - Measuring Glacier Velocity from Satellite Images, Science, 234, 1105-1108, 1986.

Manson, R., Coleman, R., Morgan, P., and King, M.: Ice velocities of the Lambert Glacier from static GPS observations, Earth, planets and space, 52, 1031-1036, 2000.

Mouginot, J., Rignot, E., Scheuchl, B., and Millan, R.: Comprehensive Annual Ice Sheet Velocity Mapping Using Landsat-8, Sentinel-1, and RADARSAT-2 Data, Remote Sens-Basel, 9, 364, 2017.

Nath, P., and Vaughan, D.: Subsurface crevasse formation in glaciers and ice sheets, J. Geophys. Res, 108, 10.1029, 2003.

Raup, B., and Scambos, T.: VELMAP. National Snow and Ice Data Center, Boulder, Colorado USA. , 2000.
Rignot, E., Mouginot, J., and Scheuchl, B.: Ice flow of the Antarctic ice sheet, Science, 333, 1427-1430, 2011.
Rott, H., Rack, W., Nagler, T., and Skvarca, P.: Climatically induced retreat and collapse of northern Larsen Ice Shelf, Antarctic Peninsula, Ann. Glaciol, 27, 86-92, 1998.
Scambos, T., Fahnestock, M., Moon, T., Gardner, A., and Klinger, M.: Landsat 8 Ice Speed of Antarctica (LISA). Center, N. N. S. a. I. D. (Ed.), NSIDC: National Snow and Ice Data Center, Boulder, Colorado USA. , 2019.
Scambos, T. A., Dutkiewicz, M. J., Wilson, J. C., and Bindschadler, R. A.: Application of Image Cross-Correlation to the Measurement of Glacier Velocity Using Satellite Image Data, Remote sensing of environment, 42, 177-186, 1992.
Scheuchl, B., Mouginot, J., and Rignot, E.: Ice velocity changes in the Ross and Ronne sectors observed using satellite radar data from 1997 and 2009, The Cryosphere, 6, 2012.
Shen, Q., Wang, H., Shum, C. K., Jiang, L., Hsu, H. T., and Dong, J.: Recent high-resolution Antarctic ice velocity maps reveal increased mass loss in Wilkes Land, East Antarctica, Scientific Reports, 8, 4477, 10.1038/s41598-018-22765-0, 2018.
Toon, O. B., and Turco, R. P.: Polar stratospheric clouds and ozone depletion, Scientific American, 264, 68-74, 1991.
van Wessem, J. M., Ligtenberg, S. R. M., Reijmer, C. H., van de Berg, W. J., van den Broeke, M. R., Barrand, N. E., Thomas, E. R., Turner, J., Wuite, J., Scambos, T. A., and van Meijgaard, E.: The modelled surface mass balance of the Antarctic Peninsula at 5.5 km horizontal resolution, The Cryosphere, 10, 271-285, 10.5194/tc-10-271-2016, 2016.
Wessel, P., Smith, W. H. F., Scharroo, R., Luis, J., and Wobbe, F.: Generic Mapping Tools: Improved Version Released, Eos Transactions American Geophysical Union, 94, 409-410, 2013.
Landsat 8 (L8) Data users handbook: https://landsat.usgs.gov/landsat-8-l8-data-users-handbook, 2016.
Zhang, S. K., Dongchen, E., Wang, Z. M., Li, Y. S., Jin, B., and Zhou, C. X.: Ice velocity from static GPS observations along the transect from Zhongshan station to Dome A, East Antarctica, Ann. Glaciol 48, 113-118, 2008.